Soft Matter

Accepted Manuscript

ROYAL SOCIETY OF CHEMISTRY

www.rsc.org/softmatter

Thermal Fluctuations of Vesicles and Nonlinear Curvature Elasticity—Implications for Size-dependent Renormalized Bending Rigidity and Vesicle Size Distribution

Fatemeh Ahmadpoor[a] **and Pradeep Sharma**[*b]

Both closed and open biological membranes noticeably undulate at physiological temperatures. These thermal fluctuations influence a broad range of biophysical phenomena, ranging from self-assembly to adhesion. In particular, the experimentally measured thermal fluctuations spectra also provides a facile route to the assessment of mechanical and certain other physical properties of biological membranes. The theoretical assessment of thermal fluctuations, be it for closed vesicles or the simpler case of flat open lipid bilayers, is predicated on assuming that the elastic curvature energy is a quadratic functional of the curvature tensor. However, a qualitatively correct description of several phenomena such as binding-unbinding transition, vesicle-to-bicelle transition, appearance of hats and saddles among others, appear to require consideration of constitutively nonlinear elasticity that includes fourth order curvature contributions rather than just quadratic. In particular, such nonlinear considerations are relevant in the context of large-curvature or small-sized vesicles. In this work we discuss the statistical mechanics of closed membranes (vesicles) incorporating both constitutive and geometrical nonlinearities. We derive results for the renormalized bending rigidity of small vesicles and show that significant *stiffening* may occur for sub-20 nm vesicle sizes. Our closed-form results may also be used to determine nonlinear curvature elasticity properties from either experimentally measured fluctuation spectra or microscopic calculations such as molecular dynamics. Finally, in the context of our results on thermal fluctuations of vesicles and nonlinear curvature elasticity, we reexamine the problem of determining the size distribution of vesicles and obtain results that reconcile well with experimental observations. However, our results are somewhat paradoxical. Specifically, the molecular dynamics predictions for the thermo-mechanical behavior of small vesicles of prior works, appear to be inconsistent with the nonlinear elastic properties that we estimate by fitting to the experimentally determined vesicle size-distribution trends and data.

1 Introduction

Biological membranes are ubiquitous in life, and form the envelope through which cells and organelles interact with their surroundings[1]. Lipid bilayers, which primarily consist of self-assembled phospholipid molecules, often form closed vesicles[2]. Usually just a few nanometers thick, the membranes serve as the gatekeepers for the cells and vesicles and aid in the transport of chemicals, facilitate mechanical and electrical signaling, transduction and adhesion. The vesicles, depending on the specific membrane composition and the surrounding environment, can exhibit a diversity of morphologies and of course serve as multi-purpose carriers that are capable of facilitating communication among cells, transporting functional genetic information as well as management of cellular waste. Aside from fundamental biological studies, lipid-based vesicles are often also created artificially in the laboratory for applications in drug design and delivery.

Although membranes are microscopically quite complex, their mechanical behavior is reasonably well-described by the phenomenological theory of elasticity and just a few continuum parameters such as the bending moduli and surface tension. Specifically, the oft-used Canham-Helfrich's theoretical framework parametrizes the energy cost of the deformation of a tension-less membrane patch by the following quadratic form[3–7*]:

$$F_b = \int_{\mathbb{S}} \frac{1}{2}\kappa_b (H - H_o)^2 + \bar{\kappa}(K - K_o) \tag{1}$$

Here κ_b and $\bar{\kappa}$ are the bending moduli that, respectively, parametrize the energy change due to changes in the mean (H) and Gaussian (K) curvatures. The corresponding spontaneous curvatures are denoted by H_o and K_o[†]. The elastic

[a] *Department of Mechanical Engineering, University of Houston, Houston, Texas 77204, USA, Email: fahmadpoor@uh.edu*
[b] *Department of Mechanical Engineering, Department of Physics, University of Houston, Houston, Texas 77204, USA, Email: psharma@central.uh.edu*

* This specific form is not quite the same as that originally presented by Canham or Helfrich. Several researchers have motivated the Helfrich-Canham Hamiltonian from fundamental grounds i.e. both as a derivation from three-dimensional solid or liquid crystal elasticity or statistical mechanics[5–7]. The specific form in Equation (1) is taken from Maleki and Fried[6] and as motivated by them, inclusion of spontaneous Gaussian curvature is important in certain situations.

† We emphasize a point which is sometimes glossed over but quite clearly highlighted by Maleki and Fried[6]. H_o can be ascribed to two contributions, geometric or constitutive. While the former corresponds to asymmetries between

energy scale is set by the bending modulus and surface tension. Their typical values are such that membranes are usually hard to stretch but bend (curve) quite easily[8,9]. Typical bending modulus of most lipid-bilayers is between 5 and 25k_BT—-small enough compared to the thermal energy scale that membranes undulate or fluctuate noticeably at physiological temperatures[8–12]. The study of these experimentally observed and widely studied thermal fluctuations has been one of the cornerstones of biophysical research on membranes[10–14]. Statistical mechanics of open (nearly) flat membranes is well-developed and, to a comparatively lesser degree of exhaustiveness, several works also exist that describe the thermal fluctuations of closed vesicles[15–19]. The reason for the interest in thermal fluctuations of membranes is simple; aside from fundamental scientific curiosity, the fluctuations have been found to be responsible for the so-called entropic (steric) repulsive force between membranes[20–23] and strongly influence phenomena such self-assembly, adhesion, binding-unbinding transitions, membrane fusion and many others[24–27]. In particular, the experimentally measured fluctuation spectra or calculated via microscopic methods such as molecular dynamics, has provided a facile route to estimate mechanical and other related properties of membranes[28–31]. For instance, in the case of a large, nearly flat membranes, the following result for the fluctuations of the out of plane displacement field h, can be easily derived based on the linearized version of the quadratic Hamiltonian described in Equation (1) : $\langle h^2 \rangle \propto k_BT/\kappa_b$[32]. This basic result has been extended to numerous other physically relevant contexts providing an avenue to extract useful information e.g. incorporation of electromechanical coupling, tilt of lipids, presence of proteins or inclusions, proximity to substrates or other vesicles among others[33–40].

For very large cells and/or vesicles, assuming that the membrane is nearly flat is a reasonable assumption and considerably simplifies the statistical mechanics analysis. However, this assumption is certainly in error for even moderately sized vesicles and may conceal some interesting physical effects due to the presence of finite curvature. For instance Morse and Milner[16] showed that the free-energy of a single vesicle *increases* logarithmically with vesicle size, if finite-size contributions are incorporated, as opposed to a logarithmic *decrease* predicted for a nearly-flat membrane. Accordingly, several works have devoted attention to the more difficult problem of understanding the fluctuation behavior of closed membranes[15–19]. In particular, one motivating factor has been the experimentally observed size-distribution of vesicles[41]. A collection of a fixed number of vesicles with different sizes can freely exchange amphiphilic molecules until a thermodynamic equilibrium state is reached. Typically, the experimentally observed size distribution of an ensemble of vesicles at equilibrium is a Gaussian in nature, with a rather large cut-off radius of about 10–20 nm. Theoretical models that purport to explain vesicle size-distribution trends, do so based on contributions from the elastic bending energy and the chemical potential of the amphiphilic molecules that is required to create a vesicle. However, such models—-which are predicated on the quadratic Helfrich Hamiltonian described in (1)—appear to be unable to completely explain all features of the experimentally observed vesicle size-distribution.

the bilayer leaflets, the latter denotes the stable equilibrium state of a membrane, which is zero for a flat membrane and can be nonzero for spherical vesicles.

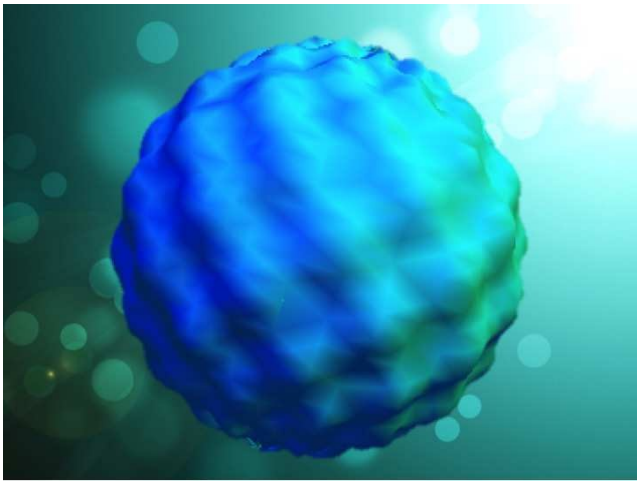

Fig. 1 A schematic showing fluctuations of a spherical vesicle. Due to the small bending stiffness of biological membranes, compared with the thermal energy scale, such vesicles undergo considerable undulations at physiological temperatures. Experimental measurement of the amplitude of the fluctuations provides a facile route to the determination of the bending stiffness of the vesicles.

Our work is motivated by the following observations and questions:

- How does the bending modulus get renormalized for high-curvature or small-sized vesicles? Ostensibly, for small vesicles, nonlinear curvature elasticity properties should play a significant role; do they indeed do so?
- In analogy with what has been done in the case of quadratic Helfrich-Canham Hamiltonian, it would also be desirable to have closed-form expressions for the thermal fluctuation spectra of nonlinear curvature elasticity to readily extract nonlinear elastic properties via experiments or molecular dynamics.
- The experimentally observed size-distributions of vesicles appear to be at odds with all theoretically derived

distributions. Helfrich speculated and (qualitatively) proposed that nonlinear curvature elasticity may play a role in the correct prediction of vesicle size-distribution. However, a derivation of vesicle size distribution that includes thermal fluctuations within a nonlinear curvature elasticity framework is still missing in the literature.

- Development of the statistical mechanics of closed membranes, incorporating fourth order nonlinear curvature elasticity, may be useful to understand various biophysical phenomena for small vesicles e.g adhesion, modification of repulsive forces, binding-unbinding among others.

To address the aforementioned issues, in the present work, we develop the statistical mechanics of closed spherical vesicles that are described by fourth order constitutively nonlinear curvature elasticity and may be suitable for the study of small-sized vesicles. The outline of the paper is as follows: Nonlinear fourth order curvature elasticity is described in Section II along with several aspects of the problem setup. The statistical mechanics of closed vesicles is developed in Section III, where we present the results for the renormalization of bending modulus of small vesicles followed by, in Section IV, the implications of our work for the assessment of size-distribution of vesicles. Our results appear to be paradoxical in light of some past computation of nonlinear elasticity properties. This, along with other issues, are discussed in the Section V where we also conclude the work.

2 Nonlinear Curvature Elasticity and Problem Setup

Consider a closed vesicle described by an enclosing surface $\mathbb{S}$. The elastic energy density may be represented by $\psi = \bar{\psi}(H,K)$. As has been discussed elsewhere[6], treatment of the vesicle surface as an isotropic fluid membrane and the foundational principles of continuum mechanics restrict the dependence of ψ solely to (H,K). Assuming conservation of area and volume, in the absence of external forces, the total potential energy of the vesicle can be written as:

$$E = \int_{\mathbb{S}} (\psi + \sigma) d\mathbb{S} + \int_V p dV \tag{2}$$

where σ and p are the surface tension and osmotic pressure, respectively. The conventional vesicle equations, as usually found in the literature, are obtained by assuming a quadratic form for ψ i.e. Equation (1). The equilibrium equations, derivable by means of variational calculus, however can proceed without the actual specification of ψ and has been carried out by a number of authors[11,42–46]. We quote below the result in the form presented by Biria et. al.[47]

$$\begin{aligned} &\bar{\psi}_H(2H^2 - K) + \frac{1}{2}\Delta_S \bar{\psi}_H + 2\bar{\psi}_K HK + 2\Delta_S(\bar{\psi}_K H) \\ &- \mathrm{div}_S(\mathbf{L}\nabla_S \bar{\psi}_K) - 2(\nabla_S H)\cdot(\nabla_S \bar{\psi}_K) - 2\bar{\psi}_K \Delta_S H \\ &- 2H(\psi + \sigma) = p \end{aligned} \tag{3}$$

Here, the subscript H (and K) denote the derivative with respect to H (and K). Further, $\mathbf{L}$ is the curvature tensor and ∇_S, Δ_S and div_S correspond to surface gradient, surface Laplacian and surface divergence operators‡, respectively[47].

Fourth order nonlinear curvature elasticity is obtaining by considering all the invariants of the curvature tensor $\mathbf{L}$ up to fourth order. Ignoring the spontaneous curvature, this leads to:

$$\bar{\psi}(H,K) = \frac{1}{2}\kappa_b H^2 + \bar{\kappa}K + \frac{1}{2}\gamma_1 H^4 + \frac{1}{2}\gamma_2 H^2 K + \frac{1}{2}\gamma_3 K^2 \tag{4}$$

where γ_i are the fourth order moduli.

In linearized curvature elasticity (i.e. the quadratic Helfrich theory), assuming that the vesicle is a sphere of radius R, the Young-Laplace equation takes the form: $R = 2\sigma/p$. In the nonlinear setting however, due to the presence of higher order moduli, this relation is modified. Assuming that sphere is the stable state, Equation (3) results in:

$$-\frac{\gamma_1}{R^5} + \frac{\gamma_3}{R^5} = p - \frac{2\sigma}{R} \tag{5}$$

which implies that for a certain range of pressure, there may be more than one sphere solution, that might be either stable or unstable depending on the values of γ_i. In this paper we will not focus on the stability of different morphologies in the context of nonlinear elasticity. It is assumed that the conditions (based on the values of surface tension, pressure and the elastic properties) ensure that a spherical vesicle is stable. For further details on this topic, the reader is referred to references[48–50].

‡ Let $\mathbf{n}$ be the normal vector to the surface $\mathbb{S}$. A surface projection tensor may be defined as:

$$\mathbf{P} = \mathbf{I} - \mathbf{n}\otimes\mathbf{n},$$

where $\mathbf{I}$ is the identity tensor. The surface gradient, surface Laplacian and surface divergence of a scalar field f and a vector field $\mathbf{g}$ can then be defined in terms of $\mathbf{P}$ and their smooth extensions f^e and $\mathbf{g}^e$ as[47]:

$$\begin{aligned} \nabla_S f &= \mathbf{P}\nabla f^e, \qquad \nabla_S \mathbf{g} = (\nabla \mathbf{g}^e)\mathbf{P}, \\ \mathrm{div}_S \mathbf{g} &= \mathbf{P}\cdot\nabla \mathbf{g}^e, \qquad \Delta_S f = \mathrm{div}_S(\nabla_S f) \end{aligned}$$

Finally, the curvature tensor takes the following form: $\mathbf{L} = -\nabla_S \mathbf{n}$.

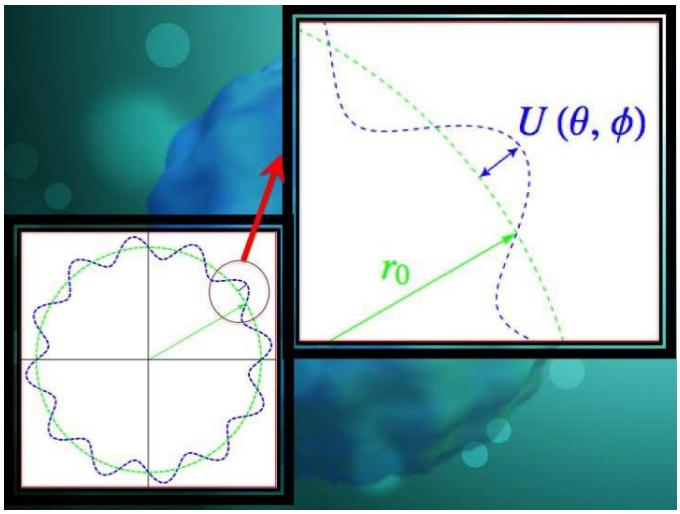

Fig. 2 Displacement field fluctuations of the surface of a spherical membrane. We have assumed that the fluctuations are normal to the surface. The fluctuating mid-plane displacement is normalized as $u(\theta,\phi) = U(\theta,\phi)/r_0$

In what follows, we will assume that the topology of the membrane does not change as it undergoes thermal fluctuations and accordingly, the contribution of the Gaussian curvature to the free energy may be neglected. [§]

§ In the conventional (linear) model, according to Gauss-Bonnet theorem, the integration of the Gaussian curvature over the surface is invariant under any deformation and hence the contribution of the Gaussian curvature to the bending energy may be ignored. This is, however a global constraint on the topology of the membrane, which is necessary but not sufficient. Strictly speaking, the Gaussian curvature at any point on the surface depends only on the metric tensor which is constrained by the intrinsic topology of the surface. To capture the effect of such strict local topological constraint, one need to fix the metric tensor's components, using local Lagrange multipliers in the total Hamiltonian. This will guarantee that the Gaussian curvature will not change at any point on the surface, and therefore all the contributions of the Gaussian curvature in the free energy can be neglected. In this manner, the total bending energy density in nonlinear framework can be modified as below:

$$\bar{\psi} = \frac{1}{2}\kappa_b H^2 + \frac{1}{2}\gamma_c H^4 + \lambda \cdot (\mathbf{g} - \mathbf{g}^0) \tag{6}$$

where γ_c is the only fourth order constant. Also, $\mathbf{g}^0$ and $\mathbf{g}$ correspond to the metric tensors of the undeformed and deformed surfaces respectively. Further, λ is a set of Lagrange multipliers accounting for the constraints on the metric tensor components. Imposing such local topological constraints, for the simplest example of an unstretchable flat sheet, it has been shown that constraining the metric tensor components results in a significant modification to the shape equation[51,52]. This notion is critical when the deformations may result in topological changes. For our specific problem, since the fluctuations are considered to take place for a fixed (*and* stable) topology– and that is a stable sphere will remain a sphere in the absence of external forces– implementing the topological constraints is unimportant. Accordingly, in the remainder of the work, the additional Lagrange multiplier term in Equation (6) is dropped.

We rescale the fourth-order moduli to emphasize the fact that nonlinear curvature elasticity introduces an intrinsic length scale—-in sharp contrast to the conventional Helfrich-theory: $\gamma_c = \kappa_b \ell_c^2$ where ℓ_c is the critical length scale that determines when the nonlinearity may be ignored, $\ell_c H \ll 1$. Typically, ℓ_c is assumed to be in the same order of magnitude as the thickness of the membrane. However, as will be elaborated in due course, there is uncertainty about the determination of this parameter and we eventually use experimental data on vesicle size-distributions to estimate that, at least for the materials system we investigated, its value is indeed of the same order as the membrane thickness. We speculate that the physical origins of ℓ_c are rooted in force and entropic interaction between adjacent lipid molecules when compelled to take highly curved configurations whose size-scale is compared to the thickness dimensions of the bilayer (and hence lipids). We will focus on the fluctuations of a closed vesicle in the shape of a perfect sphere—-as has been done by nearly all works that precede us. The fluctuating spherical vesicle (Figure. 1) with a mean radius of r_0, surface defined as $\mathbb{S} := \{\mathbf{r} \in \mathbb{R}^3 : |\mathbf{r}| = r_0\}$ has a membrane of thickness d. Consider a small but arbitrary perturbation of the surface of the vesicle. The position of each point on the *perturbed* surface of the sphere can be described as:

$$\tilde{\mathbf{r}} = \mathbf{r} + \varepsilon U \mathbf{n} \tag{7}$$

where we have assumed that the perturbation is only along the normal direction as shown in Figure. 2. Here $\varepsilon \in \mathbb{R}$ is a small number and $U(\theta,\phi) : \mathbb{S} \to \mathbb{R}$ denotes the magnitude of the normal perturbation. The mean curvature and the Jacobian of the perturbed surface can be expressed as:

$$\begin{aligned} \tilde{H} &= H + \delta H \\ \tilde{J} &= 1 + \delta J \end{aligned} \tag{8}$$

where, H is the mean curvature of the undeformed surface. Up to second order in ε, the variations of H and J may be expanded as:[45,53]

$$\begin{aligned} \delta J &= -2HU\varepsilon + (\frac{1}{2}|\nabla_S U|^2 + KU^2)\varepsilon^2 + O(\varepsilon^2) \\ \delta H &= ((2H^2 - K)U + \frac{1}{2}\Delta_S U)\varepsilon \\ &\quad + (HU\Delta_S U - \frac{1}{2}\nabla_S U \cdot (H\nabla_S U) + (4H^2 - 3K)HU^2)\varepsilon^2 \\ &\quad + O(\varepsilon^2) \end{aligned} \tag{9}$$

Neglecting the contribution of the Gaussian curvature, the bending energy per unit area of the perturbed surface can be written as:

$$\bar{\psi}[\tilde{H}] = \frac{1}{2}\kappa_b \tilde{H}^2 + \frac{1}{2}\gamma_c \tilde{H}^4 \tag{10}$$

Using Equations (8) and (9) and integrating the above expressions over the surface of the membrane, we obtain:

$$\begin{aligned}\mathscr{E}^{\text{tot}}[U,H] &= \int_{\mathbb{S}} \bar{\psi}[\tilde{H}]\tilde{J}dA_0 \\ &= \int_{\mathbb{S}} \left(E(\varepsilon^0)+E(\varepsilon^2)+E(\varepsilon^4)+O(\varepsilon^4)\right) dA_0 \quad (11)\end{aligned}$$

in which we have retained up to fourth order terms. The leading terms in the expressions for $E(\varepsilon^i)$ are as follows:

$$\begin{aligned}E(\varepsilon^0) &= \frac{1}{2}\kappa_b H^2\left(1+\ell_c^2 H^2\right) \\ E(\varepsilon^2) &= \frac{1}{8}\kappa_b(\Delta_S U)^2(1+6H^2\ell_c^2) \\ &\quad + \frac{1}{4}\kappa_b U\Delta_S U(5H^2-2K+3H^2(7H^2-4K)\ell_c^2)+\cdots \\ E(\varepsilon^4) &= \frac{1}{32}\kappa_b\ell_c^2(\Delta_S U)^4+\cdots \qquad (12)\end{aligned}$$

Specializing to the case of a perfect sphere of radius r_0, the equilibrium mean and Gaussian curvatures are $H^{-1}=-r_0$ and $K^{-1}=r_0^2$. Moreover, we define the normalized mid-plane displacement as: $u=U/r_0$. For notational simplicity, we use $\underline{\Delta} := \Delta_S(r_0=1)$ as the surface laplacian operator on the unit sphere. Assuming that θ and ϕ are polar and azimuthal angles, we can write the area element as: $dA_0 = r_0^2 d\Omega$, where $d\Omega = \sin(\theta)d\theta d\phi$. Then, integrating the terms in (12) over the area of the sphere, we obtain¶:

$$\begin{aligned}E_0 &= \int_{\mathbb{S}} E(\varepsilon^0)dA_0 = 2\pi\kappa_b\left(1+\frac{\ell_c^2}{r_0^2}\right) \\ E_2 &= \int_{\mathbb{S}} E(\varepsilon^2)dA_0 \\ &= \int_{\mathbb{S}}\left[\frac{1}{8}\kappa_b\left(1+\frac{6\ell_c^2}{r_0^2}\right)(\underline{\Delta}u)^2+\frac{3}{4}\kappa_b\left(1+\frac{5\ell_c^2}{r_0^2}\right)u\underline{\Delta}u\right]d\Omega \\ E_4 &= \int_{\mathbb{S}} E(\varepsilon^4)dA_0 = \int_{\mathbb{S}}\left[\frac{1}{32r_0^2}\kappa_b\ell_c^2(\underline{\Delta}u)^4\right]d\Omega \qquad (13)\end{aligned}$$

For notational simplicity, in what follows, we set $\kappa_1 = \frac{1}{8}\kappa_b(1+6\ell_c^2/r_0^2)$, $\kappa_2 = \frac{3}{4}\kappa_b(1+5\ell_c^2/r_0^2)$, and $\kappa_3 = \frac{1}{32}\kappa_b\ell_c^2/r_0^2$. Evidently, E_0 is the ground state energy, corresponding to the equilibrium state. A small perturbation of the surface (7), requires an additional elastic energy that can be expressed as: $E_{pert} = E_2 + E_4$. Up to second order, the energy function E_2 within the linearized curvature elasticity framework has been derived earlier by many authors. Here, we have generalized it to include the effects of constitutive nonlinearities. In the following section we will use the energy function (13) to study the thermal fluctuations of the displacement field for a spherical vesicle.

3 Thermal Fluctuations in the Context of Nonlinear Elasticity and the Renormalized Bending Rigidity of Small Vesicles

There exists a rich and extensive literature on thermal fluctuations of membranes[54–58]. In the context of lipid bilayers and biological membranes, the vast majority of the works use Helfrich's classical quadratic Hamiltonian (i.e. linearized curvature elasticity) as the starting point. Specifically, constitutive nonlinearity—as detailed in the preceding section, has hitherto not been accounted for. Unfortunately, carrying out statistical mechanics of non-quadratic Hamiltonians is a daunting task to say the least; and closed-form solutions are frequently unobtainable. The equipartition theorem, which is the essential result used by nearly all the analytical statistical mechanics works on biological membranes, is not applicable.

Several methods have been introduced in the literature for treating non-quadratic Hamiltonians. Perhaps, the most straightforward approach is the perturbation expansion[59] wherein the non-quadratic part of the Hamiltonian is considered to be a small perturbation compared to the quadratic part for which an exact solution is known. If the perturbation term is small enough, and under certain conditions, a rapid convergence of the free energy expansion may be achieved. Nevertheless, for low temperatures, divergent contributions may appear

¶ In spherical coordinates, using $(\mathbf{e}_r,\mathbf{e}_\theta,\mathbf{e}_\phi)$ as the basis vectors, the perturbed surface of the sphere is $\tilde{\mathbf{r}} = r_0(1+u(\theta,\phi))\mathbf{e}_r$ and the area element and normal vector of the perturbed surface are:

$$\begin{aligned}\tilde{J}dA_0 &= |\partial_\theta\tilde{\mathbf{r}}\times\partial_\phi\tilde{\mathbf{r}}|\ d\theta d\phi \\ &= \sqrt{1+\left(\frac{\partial u}{\partial\theta}\right)^2+\left(\frac{1}{\sin\theta}\frac{\partial u}{\partial\phi}\right)^2}\, r_0^2\sin\theta\ d\theta d\phi \\ \mathbf{n} &= \frac{\partial_\theta\tilde{\mathbf{r}}\times\partial_\phi\tilde{\mathbf{r}}}{|\partial_\theta\tilde{\mathbf{r}}\times\partial_\phi\tilde{\mathbf{r}}|}\end{aligned}$$

Also the mean curvature is:

$$\tilde{H} = -\frac{1}{2}\,\text{div}_S\ \mathbf{n}$$

The surface operators are defined as:

$$\begin{aligned}\overline{\nabla} &:= \frac{\partial}{\partial\theta}\mathbf{e}_\theta+\frac{1}{\sin\theta}\frac{\partial}{\partial\phi}\mathbf{e}_\phi \\ \underline{\Delta} &:= \frac{1}{\sin\theta}\frac{\partial}{\partial\theta}\left(\sin\theta\frac{\partial}{\partial\theta}\right)+\frac{1}{\sin^2\theta}\frac{\partial^2}{\partial\phi^2}\end{aligned}$$

The area element and the mean curvature can then be expressed as:

$$\begin{aligned}\tilde{J}dA_0 &= r_0^2(1+2u+u^2+\frac{1}{2}|\overline{\nabla}u|^2+\cdots)\sin\theta\ d\theta d\phi \\ \tilde{H} &= -\frac{1}{r_0}\left(1-u-\frac{1}{2}\underline{\Delta}u+u^2+u\underline{\Delta}u-\frac{1}{2}|\overline{\nabla}u|^2+\cdots\right)\end{aligned}$$

from second order corrections[59]. Improved results may be obtained by the so-called variational perturbation theory (VPT) which has been successfully employed to remove divergencies in several canonical problems of quantum and statistical physics[59–64]. This method is based on the so-called principle of minimum sensitivity[65] and involves the use of a trial quadratic Hamiltonian with a variational coupling parameter. The requirement that an infinite perturbation expansion series should not depend on the variational parameter, the variational coupling parameter is "optimized" so that a truncated series solution depends minimally on it. The convergence of this method has been shown to be excellent when compared to all-numerical calculations and fairly reasonable closed-form analytical solutions may be obtained with just first or second order expansions in many cases[59,60,66‖]. Renormalization group[67] (RG) is also another approach to treat the divergencies in perturbation expansions. This method is based on scaling techniques and some universal properties of materials near critical phenomena. In most of the cases, RG involves numerical calculations to estimate the free energy, and is often unable to produce analytical expressions for the correlation functions.

In what follows, we employ the variational perturbation approach and retain terms only up to the first order. Higher order corrections are cumbersome to incorporate but may be included if required. Our choice of the approach is dictated by our desire to obtain closed-form yet reasonably accurate solutions. The perturbed energy function, introduced in (13) is split in two parts; quadratic (E_2) and a non-quadratic (E_4) part that is not tractable via the equipartition theorem. We express the original Hamiltonian in the following modified form:

$$\mathbb{H}(\lambda) = \mathbb{H}_0 + \lambda \mathbb{H}_I \tag{14}$$

where λ is a control parameter, such that $0 \leqslant \lambda \leqslant 1$. We remark that $\mathbb{H}$ is *exactly* the original non-quadratic Hamiltonian when $\lambda = 1$. Also, $\mathbb{H}_0$ is a *trial* Hamiltonian, that is analytically soluble and $\mathbb{H}_I$ is the correction term. Using the concept of the canonical ensemble, the partition function is :

$$Z(\lambda) = \int \exp\left(-\beta \mathbb{H}(\lambda)\right) \mathscr{D}[u] \tag{15}$$

where $\beta = \frac{1}{k_B T}$ and $\mathscr{D}[u]$ represents the *functional integration measure*[60]. The Helmholtz free energy can be obtained as:

$$F(\lambda) = -\frac{1}{\beta} \log Z(\lambda) \tag{16}$$

Differentiating the above free-energy, with respect to λ, we obtain:

$$\begin{aligned} \frac{\partial F(\lambda)}{\partial \lambda} &= \frac{\int \mathbb{H}_I \exp(-\beta(\mathbb{H}_0 + \lambda \mathbb{H}_I)) \mathscr{D}[u]}{\int \exp(-\beta(\mathbb{H}_0 + \lambda \mathbb{H}_I)) \mathscr{D}[u]} \\ &= \langle \mathbb{H}_I \rangle \end{aligned} \tag{17}$$

The second derivative of the free-energy, with respect to λ yields:

$$\begin{aligned} \frac{\partial^2 F(\lambda)}{\partial \lambda^2} &= -\beta(\langle \mathbb{H}_I^2 \rangle - \langle \mathbb{H}_I \rangle^2) \\ &= -\beta \langle (\mathbb{H}_I - \langle \mathbb{H}_I \rangle)^2 \rangle \end{aligned} \tag{18}$$

which is always a negative value; $\frac{\partial^2 F(\lambda)}{\partial \lambda^2} \leqslant 0$. This implies that the free energy is a concave function for all values of λ, and thus, the function $F(\lambda)$ is always below the tangent to $F(\lambda)$ at $\lambda = 0$. Using the Taylor expansion around $\lambda = 0$ we can write:

$$F(\lambda) \leqslant F_0 + \left(\frac{\partial F}{\partial \lambda}\right)|_{\lambda=0} \lambda + \frac{1}{2!}\left(\frac{\partial^2 F}{\partial \lambda^2}\right)|_{\lambda=0} \lambda^2 + \cdots \tag{19}$$

We may now set $\lambda = 1$ to retrieve the free-energy corresponding to the original Hamiltonian. Also we can write the correction term in terms of the trial Hamiltonian $\mathbb{H}_0$ and the exact Hamiltonian $\mathbb{H}$ as: $\mathbb{H}_I = \mathbb{H} - \mathbb{H}_0$. The infinite Taylor series in the right hand side of Equation (19) should match the exact free energy—regardless of the choice of the trial Hamiltonian $\mathbb{H}_0$. In practice, however, the series is truncated up to a finite order M to obtain an estimate of the free energy. Let F_M be the truncated series (19) up to M-th order. Then using cumulant averages we can write the explicit form for F_M as:

$$F_{\mathrm{M}} = F_0 - \frac{1}{\beta} \sum_{k=1}^{M} \frac{(-\beta)^k}{k!} \langle [\mathbb{H} - \mathbb{H}_0]^k \rangle_{H_0}^c \tag{20}$$

where, $\langle \cdot \rangle_{\mathbb{H}_0}$ denotes the phase average with respect to $\mathbb{H}_0$ and the superscript c corresponds to cumulant averages[59**]. Unlike the infinite series expansion in Equation (19), the truncated series F_M *does* depend on the choice of the trial Hamiltonian $\mathbb{H}_0$. Accordingly, in order to obtain an optimized estimate, we need to minimize the *sensitivity* of the truncated series to the trial Hamiltonian. Suppose now that the trial Hamiltonian $\mathbb{H}_0$ in Fourier space is defined as:

‖ This approach, if only a first-order expansion is used, is also known more popularly as the Gibbs-Bogoliubov variational method which is frequently used in several classes of quantum and classical statistical mechanics problems[67–72].

** The cumulant averages of a function $\mathbb{X}$ with respect to $\mathbb{H}_0$ up to third order is defined as:[59]

$$\begin{aligned} \langle \mathbb{X} \rangle_{\mathbb{H}_0}^c &= \langle \mathbb{X} \rangle_{\mathbb{H}_0} \\ \langle \mathbb{X}^2 \rangle_{\mathbb{H}_0}^c &= \langle \mathbb{X}^2 \rangle_{\mathbb{H}_0} - \langle \mathbb{X} \rangle_{\mathbb{H}_0}^2 \\ \langle \mathbb{X}^3 \rangle_{\mathbb{H}_0}^c &= \langle \mathbb{X}^3 \rangle_{\mathbb{H}_0} - 3\langle \mathbb{X}^2 \rangle_{\mathbb{H}_0} \langle \mathbb{X} \rangle_{\mathbb{H}_0} + 2\langle \mathbb{X} \rangle_{\mathbb{H}_0}^3 \end{aligned}$$

$$\mathbb{H}_0 = \sum_{\mathbf{q}\in\mathscr{K}_N} u(\mathbf{q})G(\mathbf{q})u(\mathbf{q})^* \tag{21}$$

with $\mathbf{q}$ representing the modes of fluctuations, $u(\mathbf{q})$ being the fluctuating field in mode $\mathbf{q}$ and $G(\mathbf{q})$ is an unknown trial function that defines the form of interactions between the degrees of freedom. Then, to obtain the optimal form of $G(\mathbf{q})$, we must set:[60]

$$\frac{\partial F_M}{\partial G(\mathbf{q})} := 0. \tag{22}$$

In a rather good approximation, the result for the truncated series of the variational free energy from this method will converge i.e. $F_M \approx F_{M+1}$ and the series (20) achieves its minimal sensitivity to the trial function. We remark that restricting calculations to first order in the truncated series (20) yields just the well-known *Bogoliubov theorem*[12] for the upper bound of the exact free energy:

$$F \leqslant F_0 + \langle \mathbb{H} - \mathbb{H}_0 \rangle_{\mathbb{H}_0} \tag{23}$$

In what follows, we will use this approach up to first order to obtain a closed form solution for the free energy of the system.

As can be appreciated, the original Hamiltonian may be split into a trial and a correction term in an infinite number of ways. The next step involves choosing the optimal trial quadratic Hamiltonian. To achieve this, we start with the Fourier decomposition of the perturbation field on the sphere. To this end we expand the displacement in terms of spherical harmonics. Let N be the total number of degrees of freedom and

$$\mathscr{K}_N := \{(l,m)|(l,m) \in \mathbf{Z}\times\mathbf{Z}, l \geqslant 2, l(l+1) < N, -l < m < l\}.$$

Then we can expand the normalized perturbation field in terms of spherical harmonics as below:

$$u(\theta,\phi) = \sum_{(l,m)\in\mathscr{K}_N} u_{l,m}Y_{l,m} \tag{24}$$

where Y_{lm}[††] are spherical harmonics[73] with eigenvalues:

$$\nabla^2 Y_{l,m} = -q_{l,m}^2 Y_{l,m} = -l(l+1)Y_{l,m} \tag{25}$$

and $u_{l,-m} = u_{l,m}^*$ are the Fourier transformation of $u(\theta,\phi)$:

$$u_{l,m} = \int_{\mathbb{S}} u(\theta,\phi)Y_{lm}^* d\Omega \tag{26}$$

We select the general form for the quadratic trial Hamiltonian $\mathbb{H}_0$ in Fourier space as defined in Equation (21). The goal now is to match the exact free-energy as closely as possible by finding an optimal match for the form of the propagator $G(\mathbf{q})$. To this end we set:[12,60]

$$\frac{\partial}{\partial G(\mathbf{q})}\left(F_0 + \langle \mathbb{H} - \mathbb{H}_0 \rangle_{\mathbb{H}_0}\right) := 0 \tag{27}$$

The partition function and the free energy corresponding to the trial quadratic Hamiltonian $\mathbb{H}_0$ in Equation (21) is obtained as:

$$\begin{aligned} Z_0 &= \int e^{-\beta\mathbb{H}_0[u]}\mathscr{D}[u], \\ F_0 &= \alpha_F + \frac{k_B T}{2}\sum_{\mathbf{q}\in\mathscr{K}_N}\log(G(\mathbf{q})) \end{aligned} \tag{28}$$

where α_F is a constant independent of the propagator $G(\mathbf{q})$. Calculating F_0 from (28) and substituting it into the L.H.S. of Equation (23), we obtain the variational free energy F_{var} as:

$$\begin{aligned} F_{\text{var}} &= F_0 + \langle \mathbb{H} - \mathbb{H}_0 \rangle_{\mathbb{H}_0} \\ &= \alpha_F + \frac{k_B T}{2}\sum_{\mathbf{q}\in\mathscr{K}_N}\log(G(\mathbf{q})) \\ &+ \sum_{\mathbf{q}\in\mathscr{K}_N}(\kappa_1\mathbf{q}^4 - \kappa_2\mathbf{q}^2)\langle u(\mathbf{q})^2\rangle_{\mathbb{H}_0} \\ &+ 4\pi\kappa_3\langle(\nabla^2 u)^4\rangle_{\mathbb{H}_0} \end{aligned} \tag{29}$$

The mean square value of the perturbation field in each mode of the fluctuation can be obtained using the equipartition theorem[74]:

$$\langle u(\mathbf{q})^2\rangle_{\mathbb{H}_0} = \frac{k_B T}{2G(\mathbf{q})} \tag{30}$$

†† We have excluded the modes corresponding to $l = 0$ and $l = 1$, since these modes represent the area change and the rigid body motion of the vesicle and hence do not contribute to the total energy. We also recall the two important properties of the spherical harmonics, which will be used later in our calculations. They are orthonormal:

$$\int_{\mathbb{S}} Y_{lm}Y_{l'm'}^* d\Omega = \delta_{ll'}\delta_{mm'}$$

and separable:

$$Y_{lm} = P_l^m(\theta)e^{im\phi}$$

where $P_l^m(\theta)$ is the Legendre polynomial corresponding to the mode (l,m). In what follows, for the eigenvalues of the spherical harmonics, we use the notation $\mathbf{q} = q_{l,m}$ wherein $\mathbf{q}^2 = q_{l,m}^2 = l(l+1)$.

Also the last term in (29) which is a higher order correlation function, may be calculated by invoking Wick's theorem[74]:

$$\langle(\nabla^2 u)^4\rangle_{\mathbb{H}_0} = 3\langle(\nabla^2 u)^2\rangle^2_{\mathbb{H}_0} \tag{31}$$

Minimization of the variational free energy in (29) with respect to the unknown propagator $G(\mathbf{q})$ provides an upper bound for the exact free energy. Then, solving Equation (27) gives us the following form for $G(\mathbf{q})$:

$$G(\mathbf{q}) = \left((\kappa_1 + 24\pi\eta\,\kappa_3)\mathbf{q}^2 - \kappa_2\right)\mathbf{q}^2 \tag{32}$$

where,

$$\eta = \langle(\nabla^2 u)^2\rangle_{\mathbb{H}_0} = \frac{1}{4\pi}\sum_{\mathbf{q}\in\mathscr{K}_N}\mathbf{q}^4\langle u(\mathbf{q})^2\rangle_{\mathbb{H}_0} \tag{33}$$

which should be calculated by integrating over all undulation modes. For brevity we rewrite Equation (32) as:

$$G(\mathbf{q}) = \frac{1}{8}(c_1\mathbf{q}^4 - c_2\mathbf{q}^2) \tag{34}$$

where c_1 and c_2 are the corresponding coefficients of $\mathbf{q}^4$ and $\mathbf{q}^2$ in (32), respectively. The unknown value of η in the expression for c_1, should be calculated from the implicit equations of (30), (32) and (33):

$$\begin{aligned}\eta &= \frac{1}{4\pi}\sum_{\mathbf{q}\in\mathscr{K}_N}\mathbf{q}^4\langle u(\mathbf{q})^2\rangle_{\mathbb{H}_0}\\ &= \frac{k_BT}{4\pi}\sum_{\mathbf{q}\in\mathscr{K}_N}\frac{\mathbf{q}^4}{2G(\mathbf{q})}\\ &= \frac{k_BT}{\pi c_1}\sum_{\mathbf{q}\in\mathscr{K}_N}\left(1+\frac{c_2}{c_1\mathbf{q}^2}+\cdots\right)\end{aligned} \tag{35}$$

where, to further simplify our calculations, we have dropped the term $\frac{1}{\mathbf{q}^2}$ since it is negligible compared to one– $\mathbf{q}^2 \gg 1$. To compute the summation we replace it with an integral:

$$\sum_{\mathbf{q}\in\mathscr{K}_N} := \sum_l (2l+1) \approx \int (2l+1)dl \tag{36}$$

where l_{max} can be easily obtained from the total number of modes (degrees of freedom):

$$N = \sum_l (2l+1) = \frac{4\pi r_0^2}{A_0} \tag{37}$$

in which A_0 is the area associated with each degree of freedom, and is typically of the same order of magnitude as d^2 with d is the thickness of the membrane. Substituting the solution of Equation (35) for η into the expression for $G(\mathbf{q})$ in Equation (34) gives us the following form for the coefficients c_1 and c_2:

$$\begin{aligned}c_1 &= \frac{1}{2}\kappa_b\left(1+\frac{6\ell_c^2}{r_0^2}+\chi\right)\\ c_2 &= 6\kappa_b\left(1+\frac{5\ell_c^2}{r_0^2}\right)\end{aligned} \tag{38}$$

where,

$$\chi = \sqrt{1+\frac{12\ell_c^2}{r_0^2}+\frac{36\ell_c^4}{r_0^4}+\frac{24\ell_c^2 N}{\beta\kappa_b r_0^2}} \tag{39}$$

Note that the $\mathbf{q}^4$ contribution in (32) is equivalent to the bending rigidity (c_1) of a vesicle studied in the context of linearized curvature elasticity, and according to (38), can be significantly larger than the bare modulus κ_b. We also note that there is a curvature-dependent suppression of thermal fluctuations in the nonlinear context and accordingly larger vesicles experience stronger fluctuations, compared to smaller vesicles. On the other hand, the $\mathbf{q}^2$ term in Equation (34) has softening effects, that arise from geometric nonlinearities. In the remainder of this section, we aim to study the softening effects of the thermal fluctuations on the bending rigidity. This topic has been well appreciated since the early and pioneering work by Helfrich[56,75–77]. Considering geometric nonlinearity and using first order approximations, Helfrich[75] explained that the renormalized bending rigidity in linearized curvature elasticity (for nearly flat membranes) can be written as:‡‡

$$\kappa_{\text{eff}} = \kappa_b + \frac{\alpha}{2\pi}k_BT\log N \tag{40}$$

wherein α is a universal constant and N is the number of molecules in the system. Assuming weak rippling in nearly flat membranes, he predicted $\alpha = -1$. Peliti and Leibler[56] also reexamined this problem and obtained α as -3. Later on, Kleinert[77] rigorously discussed the origins of these discrepancies and highlighted the care needed in choosing the integration measures in path integrals as well as some algebraic errors in expanding the energy formulation in terms of the fluctuation field. He confirmed that $\alpha = -3$. In the following, we will revisit this problem to study the coupled effects of geometric

‡‡ We highlight that in many works on this topic, the bending energy density is assumed to have the form of $\frac{1}{2}\kappa_b'(1/R_1+1/R_2)^2$ in which R_1 and R_2 are the principle curvatures radiuses. In this form, the mean curvature is considered to be: $H' = 1/R_1+1/R_2$, while in the present work, we consider half of this value as mean curvature— $H = (1/R_1+1/R_2)/2$. Accordingly, the bending energy of a sphere, based on our assumption is obtained as: $2\pi\kappa_b$, while in some works, the bending energy is assumed to be $8\pi\kappa_b'$. Therefore, the change in the bending modulus in some of the references we have cited is: $\frac{\alpha}{8\pi}k_BT\log N$. A comparison between these two forms, shows that any variation in κ_b, used in our model, is four times larger than those in other works.[56,75–77]

and constitutive nonlinearities. We note in passing that, in a somewhat controversial and later work,[76], argued for the use of *curvature* as the proper integration measure and obtained $\alpha = +1$. This result is however widely disputed.

Consider now a spherical vesicle (described by linearized elasticity) with a bending rigidity of c_1 and radius r_0. The bending energy can be computed to be: $\int \frac{1}{2} c_1 \frac{1}{r_0^2} dA_0 = 2\pi c_1$. Also, at finite temperature, the free energy of the vesicle can be obtained using Equations (28) and (34):

$$\begin{aligned} F_0 &= -k_B T \log Z_0 \\ &= \alpha_F + \frac{k_B T}{2} \sum_{\mathbf{q}\in\mathscr{K}_N} \log G(\mathbf{q}) \\ &= \alpha_F + \frac{k_B T}{2} \sum_{\mathbf{q}\in\mathscr{K}_N} \left(\log c_1 \mathbf{q}^4 - \frac{c_2}{c_1 \mathbf{q}^2} + \cdots \right) \end{aligned} \tag{41}$$

The above expression shows that contribution of geometric nonlinearity, produces additional terms in the Taylor expansion of the free-energy. The "additional free energy" can be interpreted as the change in apparent bending stiffness:

$$\begin{aligned} \Delta F &= \frac{1}{2} k_B T \sum_{\mathbf{q}\in\mathscr{K}_N} \left(\frac{c_2}{c_1 \mathbf{q}^2} + \frac{c_2^2}{2 c_1^2 \mathbf{q}^4} + \cdots \right) \\ &:= 2\pi (c_1 - \kappa_{\text{eff}}) \end{aligned} \tag{42}$$

Thus, the effective bending stiffness, can be calculated up to first order as:

$$\kappa_{\text{eff}} = c_1 - \frac{c_2}{4\pi c_1} k_B T \sum_{\mathbf{q}\in\mathscr{K}_N} \frac{1}{\mathbf{q}^2} \tag{43}$$

The summation is calculated using integration over all possible modes:

$$\begin{aligned} \sum_{\mathbf{q}\in\mathscr{K}_N} \frac{1}{\mathbf{q}^2} &= \int \frac{2l+1}{l(l+1)} dl \\ &= \log N \end{aligned} \tag{44}$$

Substituting the above integral into Equation (43), we obtain the effective bending rigidity as:

$$\kappa_{\text{eff}} = \frac{1}{2} \kappa_b \left(1 + \frac{6\ell_c^2}{r_0^2} + \chi \right) - \frac{\alpha'}{4\pi} k_B T \log N \tag{45}$$

where χ has been previously defined in (39) and α' is:

$$\begin{aligned} \alpha' &= \frac{c_2}{c_1} \\ &= \frac{12 + \frac{60\ell_c^2}{r_0^2}}{1 + \frac{6\ell_c^2}{r_0^2} + \chi} \end{aligned} \tag{46}$$

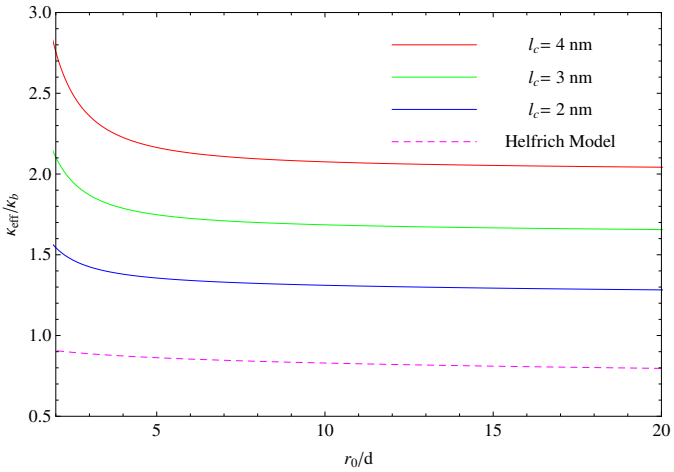

Fig. 3 Renormalized bending modulus for different values of ℓ_c. Solid red, green and blue correspond to $\ell_c = 4$nm, $\ell_c = 3$nm and $\ell_c = 2$nm, respectively. Dashed line is obtained from Helfrich linear model in which $\ell_c = 0$. The data has been calculated with $\kappa_b = 20 k_B T$ and $d = 5$nm.

Note that in the limit of $\ell_c \to 0$ the above expression reduces to that of conventional linearized curvature elasticity model[77]. For quantitative comparisons, we have calculated the bending stiffness, for a range of vesicle size with different values of ℓ_c. The results are shown in Figure. 3 where we compare four different cases. The horizontal axis is the normalized radius of the vesicle r_0/d where we set $d = 5$nm. Solid blue, green and red lines correspond to $\ell_c = 2$nm, $\ell_c = 3$nm and $\ell_c = 4$nm, respectively. The dashed line corresponds to the case of $\ell_c = 0$ which reduces to Helfrich quadratic model[75]. As can be readily observed, for small vesicles that have high curvatures, the effect of nonlinearity become quite significant. Even for a small value of $\ell_c = 3$nm—less than the typical thickness of the membrane—the apparent bending rigidity becomes significantly *stiffer* for sub-20 nm vesicles. Also, the effect of nonlinearity does not vanish in the limit of the flat membrane, when $H \to 0$. The corresponding limits of the normalized effective bending rigidity $\kappa_{\text{eff}}/\kappa_b$ for the cases of $\ell_c = 2$nm, $\ell_c = 3$nm and $\ell_c = 4$nm are found to be 1.42, 1.76 and 2.13, respectively.

4 Size Distribution of Vesicles

Vesicles can be artificially made across a broad range of diameters. However, if an ensemble of vesicles are allowed to freely exchange molecules—artificial or nature-made—the size of the vesicles will change for some period, until they become thermodynamically stable. At this state, it is very un-

likely to find vesicles beyond certain sizes, i.e. there is discernible maximum and minimum size-limit for the radius of the vesicles. Depending on the experimental methods used for the preparation of vesicles, these size limits may slightly vary in the beginning, but eventually the experimentally observed size distributions appear to become independent of the method of preparation and are determined by macroscopic mechanical and entropic properties of the vesicles[78]. Several experimental efforts have been dedicated to this subject[78–80]. The most common method to determine the size distribution of vesicles is via dynamic light scattering (DLS) measurements. Another well-known method is to use cryo-TEM images[81–83] and obtain the size distribution histogram using statistical analysis. In a recent work Xu et. al.[41] have used a combination of these two approaches and obtained the size distribution for a set of lauric acid vesicles. They confirmed that the size of the vesicles is distributed within a finite range with a remarkably large cut-off radius of about $20nm$. In this section, using the results derived in the preceding sections, we aim to study the qualitative effects of mechanical properties and their corresponding entropic effects on the size distributions of small unilamellar vesicles.

In the following we assume that the vesicles can exchange amphiphilic molecules, while the total number of the vesicles remains fixed. Also the spontaneous curvature is considered to be zero, and that there is always non-zero amount of energy cost for any non-zero curvature. Given that N is the number of amphiphilic molecules in a vesicle, the size distribution of the vesicles, $w(N)$ is determined by the total free energy F and the Boltzmann factor:

$$w(N) \propto \exp(-F/k_BT) \tag{47}$$

We first briefly review the predictions for Equation (47) made by conventional approaches before discussing the results unique to this work.

The bending energy of a sphere in linearized curvature elasticity is alway: $2\pi\kappa_b$ which is independent of the vesicle size. This implies that regardless of the size of two vesicles, the transfer of surfactant molecules from one vesicle to another does not change the total bending energy. This, results in a flat distribution for the vesicles' sizes (47). The total free energy for the vesicle with N number of amphiphilic molecules and chemical potential μ can then be written as:

$$F = 2\pi\kappa_b + N\mu \tag{48}$$

Equation (48) gives rise to an exponentially decaying distribution, with *zero* size, being the most probable size—a rather glaring problem. To further modify the result of Equation (47), Helfrich[84] proposed to include the entropic effects in the elastic energy. As discussed in the last section, in the conventional linear framework, the thermal undulations lead to softening effects on the effective bending modulus[75]. The corresponding effective bending modulus is provided in Equation (40). To account for the entropic effects, Helfrich[84] substituted the bare value of bending modulus κ_b by the renormalized bending stiffness κ_{eff}:

$$w(N) \propto \exp\left(\frac{-\mu N - 2\pi\kappa_{\text{eff}}}{k_BT}\right) \tag{49}$$

The above expression has been extensively used to predict the size distribution of the vesicles. In general, using the expression for the effective bending rigidity (40), the following size distribution is obtained:

$$w(N) \propto N^{-\alpha}\exp(-\mu N/k_BT) \tag{50}$$

The major differences between prior theoretical works on this topic, arise from the diversity in predicting the universal constant α. Using $\alpha = -1$ and normalizing the size distribution to 1, Helfrich[84] obtained the size distribution as:

$$w(N) = \left(\frac{2}{\overline{N}}\right)^2 N\exp\left(-\frac{2N}{\overline{N}}\right) \tag{51}$$

where $\overline{N}$ is the mean number of molecules per vesicle and is determined by the chemical potential μ. As well-evident, the final distribution function described in Equation (51) is *independent* of the mechanical properties of the vesicles. Furthermore, since the vesicles cannot deform beyond a certain curvature and there is always a cut-off radius for the size distribution of the small vesicles, such a distribution is not compatible with experimental observations. To resolve the inconsistency, Helfrich[84] suggested that fourth order curvature elasticity terms should be incorporated in the bending energy formulation. Using a rather crude approximation, he demonstrated that accounting the fourth order term can alter the size distribution to make smaller sizes less probably. He modified the probability density distribution in the following form:

$$w(N) \propto Ne^{-AN-B/N} \tag{52}$$

The above distribution although slightly shifts the mean value of the diagram to a larger size, and suggests smaller probability for smaller sizes, is incapable of predicting the correct value for the experimentally observed cut-off radius.

In a different work, Morse and Milner[16] suggested that the free energy, due to translational and rotational entropy, increases logarithmically with the size of the vesicle in the following form:

$$F(N) = F_0 + \alpha k_BT\log N \tag{53}$$

We note that in the present work for pure lipid membranes, we assume that there is no entropic contributions from tilting or area change.

Table 1 Comparison between the previous models of size distribution and the present work. In general, the distribution function can be expressed as: $w(N) \propto N^{\zeta} \exp(-f(N))$. The second column in this table shows various values for the exponent ζ in different models. Also, various forms of the function $f(N)$ are shown in the third column. The symbols A and B are constants, representing the chemical potential and those associated with fourth order moduli, respectively. Further, A_i in the last row are constants, corresponding to coefficients of renormalized bending stiffness in the present model. A comparison between the listed models, shows that Helfrich nonlinear model and the present model provide more realistic predictions of the cut-off radius in the size distribution of vesicles. Unlike Helfrich's nonlinear model, in the present work, the entropic effects of the constitutive nonlinearity, are taken into account to further modify the predicted size distribution.

Model	ζ	$f(N)$	Cut-off radius (r_c)
E=$2\pi\kappa_b + \mu N$	$\zeta = 0$	AN	$r_c = 0$
Helfrich linear model: Eq.(51)	$\zeta = 1$	AN	$r_c = 0$
Helfrich nonlinear model: Eq. (52)	$\zeta = 1$	$AN + B/N$	$r_c > 0$
Morse and Milner: Eq. (54)	$\zeta = -7/8$	AN	$r_c = 0$
Kleinert: Eq. (55)	$\zeta = 4/3$	AN	$r_c = 0$
Present model: Eq. (58)	$\zeta \leqslant 3$	$A_0 N + A_1/N + \sqrt{A_2 + A_3/N + A_4/N^2}$	$r_c > 0$

for which they evaluate $\alpha = +\frac{7}{8}$. Based on this, they obtained the size distribution as:

$$w(N) \propto N^{-7/8} e^{-\mu N} \tag{54}$$

Unfortunately, this predicted size-distribution renders smaller vesicles more probably not less and is somewhat contradictory to the experimental observation that there exists a minimal vesicle size.

Finally, we note that Kleinert[53] also revisited this problem. Renormalizing the mean and Gaussian and spontaneous curvature constants, and considering their effects together within a harmonic approximation, he obtained the following form for the size distribution:

$$w(N) \propto N^{7\rho^2 - 6\rho + 4/3} e^{-AN} \tag{55}$$

in which he introduced the so called *elastic fraction* $\rho \in (0,1)$ that essentially captures the combined entropic effects of mean, Gaussian and spontaneous curvatures. It can be readily seen that the exponent of N has a maximum of $7/3$. Nevertheless for pure bending of the lipid membranes that does not involve any tilt or area change, the maximum is found to be $4/3$. As a result, compared to (51) and (54) the distribution (55) predicts smaller probability for small sizes, however, is still far from the experimental observations.

We now turn to the use of the thermal fluctuations results we have derived in the preceding section, in the context of fourth order nonlinear elasticity, to derive the size-distribution. Consider the following general form of the size distribution:

$$w(N) \propto N^{\zeta} \exp(-f(N)) \tag{56}$$

wherein ζ and $f(N)$ determine different forms of the distributions and their dependences on N in various models. Prior models as well as ours (to be described) may be described by appropriate specification of ζ and $f(N)$.

In our model, substituting Equation (45) into Equation (48), the total free-energy for a given size of the vesicle can be written as:

$$\begin{aligned} F &= 2\pi\kappa_{\text{eff}} + \mu N \\ &= \pi\kappa_b \left(1 + \frac{6\ell_c^2}{r_0^2} + \chi\right) - \frac{\alpha'}{2} k_B T \log N + \mu N \end{aligned} \tag{57}$$

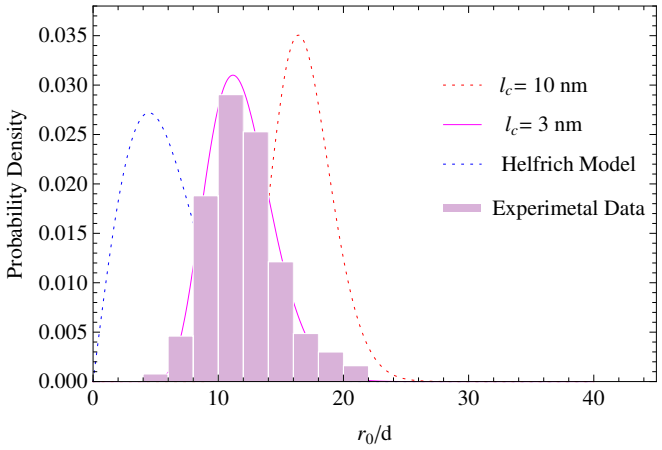

Fig. 4 Size distribution of vesicles with different values of ℓ_c. In this figure, the horizontal axis is the normalized radius of the vesicle $\xi = r_0/d$ and the vertical axis is the probability of finding vesicles within a certain radius. Dotted blue curve corresponds to the size distribution as predicted by linear curvature elasticity[84]. The solid magenta is obtained assuming $\ell_c = 3$nm, which results in a shift in the size distribution, to larger sizes. Also the dotted red line corresponds to $\ell_c = 10$nm which dramatically changes the cut-off radius as well as the mean radius of the vesicles. Based on the experimental data[41], shown in purple color, we have estimated the characteristic length for this kind of lauric acid vesicles to be about $\ell_c = 3$nm. For our calculations, we have set $\kappa_b = 20k_BT$ and $d = 5$nm.

where χ and α' are defined in (39) and (46) respectively. Using Equation ((49)) we propose the following size-distribution:

$$w(N) \propto N^{\alpha'/2} \exp\left(-f(N)\right) \tag{58}$$

where

$$f(N) = \frac{1}{k_BT}\left(\mu N + \frac{A_1}{N} + \sqrt{A_3 + \frac{A_4}{N} + \frac{A_5}{N^2}}\right) \tag{59}$$

Here we have substituted r_0^2 in (57) by $NA_0/4\pi$ where A_0 is the area per amphiphilic molecule. Other A_i are coefficients that depend on κ_b and ℓ_c. Note that the exponent α' in Equation (58) is not a *constant* and varies with the radius of the vesicle. On the other hand, in addition to the term $1/N$, the contribution of the term $1/\sqrt{N}$ in the exponential function dramatically reduces the probability for finding small vesicles. These two effects together result in a notable shift in the size-distribution diagram towards larger sizes when compared to other models[16,53,84].

A comparison between the results of our model with experimental data[41] is made in Figure. 4, where we have plotted the size distribution for three different cases. In this figure, the horizontal axis is the normalized radius of the vesicle r_0/d and the vertical axis is the probability of finding vesicles with a certain radius. Dotted blue curve corresponds to the size distribution within linear curvature elasticity[84] as presented in Equation (51). The solid magenta is obtained from the present nonlinear model, assuming $\ell_c = 3$nm and the dotted red line corresponds to $\ell_c = 10$nm. Finally, we may estimate the characteristic length ℓ_c to fit our results to those obtained from the experiments. A comparison between our results and experimental data[41] in Figure. 4 shows that the corresponding characteristic length for this type of composition is roughly about $\ell_c = 3$nm. Even though this value is in the same order as the thickness of the membrane, at finite temperature it can dramatically change the size distribution of the vesicles through thermal fluctuations. Finally, the experimentally observed cut-off radius is clearly evident in our model.

5 Discussion and Concluding Remarks

One of the main results derived in this paper is a closed-form expression for the spectra of the thermal fluctuations of spherical vesicles duly incorporating nonlinear curvature elasticity terms. In conjunction with our results, either molecular dynamics simulations or experimental flicker spectroscopy may now be used to extract nonlinear elasticity properties. The renormalized bending rigidity due to thermal fluctuations is found to be size-dependent and a dramatic stiffening is predicted to occur for small sub-20 nm vesicle sizes.

The conventional models (based on linear curvature elasticity) that purport to describe vesicle size-distributions typically fail to adequately capture a few qualitative aspects of the distribution for small vesicle sizes. We have used our analytical expression for the renormalized bending stiffness in the nonlinear framework, to study the size distribution of vesicles. Although, all the existing models predict a Gaussian size distribution, the problem of the cut-off radius–below which the vesicles are not likely to exist– is inadequately predicted and as evident from our predictions, the size-distribution is considerably more complex. A possible explanation for the instability of vesicles with sizes below the cut-off radius is the entropic repulsive forces between the amphiphilic molecules.

In the following we summarize the key issues related to fourth-order moduli as discussed in prior works put in the context of what we have found:

- The first one is regarding the magnitude and significance of the fourth order modulus. Typically ℓ_c is assumed to be of the order of the thickness of the membrane. Based on this assertion, the higher order con-

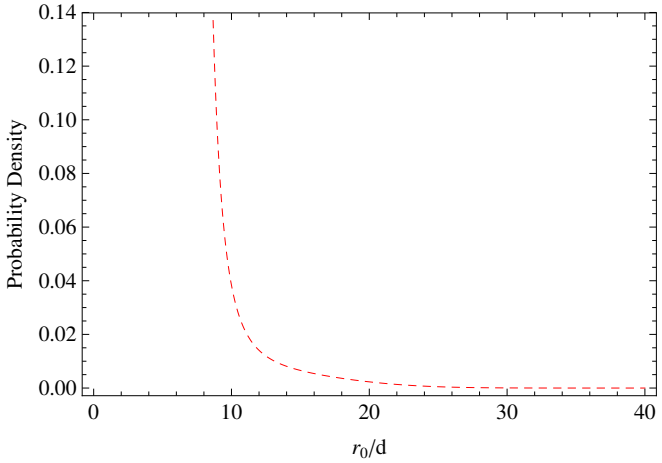

Fig. 5 Size distribution of vesicles with negative fourth order modulus is shown qualitatively in this figure. In sharp contrast to experimental observations known so far, the distribution is discontinuous and is not a Gaussian distribution. Small-size vesicles are *more* probable not less. Finally, beyond a certain size, the vesicle becomes unstable. This plot is obtained by $\ell_c = 2$nm. For larger values of ℓ_c, the unstable region is shifted to larger sizes.

tributions of the bending energy are usually ignored in studying the mechanical response of the vesicles. Our results, however, demonstrate that thermal fluctuations of small unilamellar vesicles are significantly influenced by the higher order modulus even for small values of ℓ_c. Furthermore, for nearly flat membranes, wherein the curvature dependency vanishes, the nonlinearity can still significantly suppress the undulations and hence increase the apparent rigidity. For example, using $\ell_c =$ 2nm which is less than the thickness of the membrane, a correction of about 40% is obtained in the apparent bending rigidity. In order to highlight some of the discrepancies between our results with the prior works the reader is referred to a recent work by Harmandaris and Deserno[85]. Using molecular dynamics simulations, these authors employed the well-known idea of tether-pulling experiments[86,87] to study the fourth order correction of the bending energy for cylindrical vesicles consist of pure DPPC lipid molecules. Their results indicate that the quadratic energy function proposed by Helfrich is valid for a wide range of curvature radii up to the thickness of the membrane. The entropic effects are assumed to be intrinsically embedded in the simulations. Nevertheless, we speculate that, for tethered membranes, due to the high surface tension, the undulations are significantly suppressed and hence the role of entropic effects in the apparent bending stiffness were not adequately taken into account. This can be explained by recognizing the fact that the fluctuations of the out of plane displacement field in the presence of surface tension vary as: $\langle h^2 \rangle \propto 1/\sigma$. According to the relation between the surface tension and the radius of the vesicle $R \propto 1/\sqrt{\sigma}$, to reduce the size of the vesicle to just a few times of the thickness of the membrane, a relatively high tension field is required to overcome the entropic effects. It has been observed in experiments that if such tension field is abruptly removed, the vesicle will undergo an entropic instability[88].

In a different work Li et. al.[89], also using molecular dynamic simulations, have computed the elastic properties of the membrane, including fourth order moduli. Unlike the work by Harmandaris and Deserno[85], these authors carried the their simulations for various volume fractions of hydrophilic molecules. Interestingly, their results on free energy calculation also demonstrate that the higher order contribution of bending energy, is relatively small and the difference between their results and those obtained within Helfrich model is no more than 10%. Also, they obtained values for the fourth order moduli which surprisingly depend on the topology of the vesicles– negative values for spherical and positive values for cylindrical vesicles. This is puzzling to us since the properties, in principle, or for the underlying material not a topological structure. A possible explanation for observation of such contradictory results in their analysis is that the contribution of the intrinsic topology— spontaneous Gaussian and mean curvatures— is not taken into account. Strictly speaking, a flat membrane does not transform to spherical shape, unless an energy cost is considered for fission or fusion. In this manner all the free energy should not be referred to only bending energy. Hence, the free energy of cylindrical and spherical shapes should be analyzed using the different reference states.

- The second issue regarding the fourth order modulus is related to the *sign* of the modulus. In the present work, the higher order modulus is assumed to be positive from the outset. However, it has been argued that the fourth order modulus is negative when dealing with different co-surfactants[90]. Also it has been argued that a negative fourth order elastic modulus is a possible explanation for the mechanism of lipid protein sorting[91]. We note that, in the presence of different compositions, various stable phases might be observed that can be described in terms of different spontaneous mean and Gaussian curvatures or alternatively different bending stiffnesses. We however, believe that a change in the molecular structure of the membrane, results in both mechanical and

topological transformations. For pure lipid membranes, a positive fourth order correction of bending energy is required to explain the experimentally observed size distribution of vesicles—as evident from Figure. 5 which clearly demonstrates how unrealistic the size-distribution results will be if a negative fourth order modulus is used.

- Finally, we note that that, when the area-size of the membrane becomes comparable with its thickness, the notion of high-q cutoff necessary in the functional integration becomes dubious. For the smallest size vesicles, we come dangerously close to that limit. However, given the close agreement of our results with experimentally observed vesicle size-distributions, we speculate that our results are at least qualitatively reasonable.

Acknowledgements

FA gratefully acknowledges discussions with Professor Gemunu Gunaratne. PS acknowledges financial support from the University of Houston M.D. Anderson Professorship.

References

1 Singer, S. J., and Garth L. Nicolson. The fluid mosaic model of the structure of cell membranes. Day and Good Membranes and viruses in immunopathology (1972): 7-47.

2 Israelachvili, Jacob N., D. John Mitchell, and Barry W. Ninham. Theory of self-assembly of lipid bilayers and vesicles. Biochimica et Biophysica Acta (BBA)-Biomembranes 470.2 (1977): 185-201.

3 Canham, Peter B. The minimum energy of bending as a possible explanation of the biconcave shape of the human red blood cell. Journal of Theoretical Biology 26.1 (1970): 61-81.

4 Helfrich, W. Elastic properties of lipid bilayers: theory and possible experiments. Zeitschrift fr Naturforschung. Teil C: Biochemie, Biophysik, Biologie, Virologie, 28(11), 693. 1973

5 Steigmann, D. J. Fluid films with curvature elasticity. Archive for Rational Mechanics and Analysis 150.2 (1999): 127-152.

6 Maleki, Mohsen, Brian Seguin, and Eliot Fried. Kinematics, material symmetry, and energy densities for lipid bilayers with spontaneous curvature. Biomechanics and modeling in mechanobiology 12.5 (2013): 997-1017.

7 Deserno, Markus. Fluid lipid membranes: From differential geometry to curvature stresses. Chemistry and physics of lipids 185 (2015): 11-45.

8 Nelson, Philip. Biological physics. New York: WH Freeman, 2004.

9 Phillips, Rob, et al. Physical biology of the cell. Garland Science, 2012.

10 Lipowsky, Reinhard. The conformation of membranes. Nature 349.6309 (1991): 475-481.

11 Seifert, Udo. Configurations of fluid membranes and vesicles. Advances in physics 46.1 (1997): 13-137.

12 Safran, Samuel A. Statistical thermodynamics of surfaces, interfaces, and membranes. Vol. 90. Perseus Books, 1994.

13 Piran, Tsvi. Statistical mechanics of membranes and surfaces. World Scientific, 2004.

14 Podgornik, Rudi, and V. Adrian Parsegian. Thermal-mechanical fluctuations of fluid membranes in confined geometries: the case of soft confinement. Langmuir 8.2 (1992): 557-562.

15 Schneider, M. B., J. T. Jenkins, and W. W. Webb. Thermal fluctuations of large quasi-spherical bimolecular phospholipid vesicles. Journal de Physique 45.9 (1984): 1457-1472.

16 Morse, D. C., and S. T. Milner. Fluctuations and phase behavior of fluid membrane vesicles. EPL (Europhysics Letters) 26.8 (1994): 565.

17 Morse, David C., and Scott T. Milner. Statistical mechanics of closed fluid membranes. Physical Review E 52.6 (1995): 5918.

18 Michalet, Xavier, David Bensimon, and Bertrand Fourcade. Fluctuating vesicles of nonspherical topology Physical review letters 72.1 (1994): 168.

19 Seifert, U. The concept of effective tension for fluctuating vesicles. Zeitschrift fr Physik B Condensed Matter 97.2 (1995): 299-309.

20 Helfrich, W. S. R. M., and R-M. Servuss. Undulations, steric interaction and cohesion of fluid membranes. Il Nuovo Cimento D 3.1 (1984): 137-151.

21 Janke, W., and H. Kleinert. Fluctuation pressure of membrane between walls. Physics Letters A 117.7 (1986): 353-357.

22 Freund, L. B. Entropic pressure between biomembranes in a periodic stack due to thermal fluctuations. Proceedings of the National Academy of Sciences 110.6 (2013): 2047-2051.

23 Sharma, Pradeep. Entropic force between membranes re-examined. Proceedings of the National Academy of Sciences 110.6 (2013): 1976-1977.

24 Lipowsky, Reinhard, and Udo Seifert. Adhesion of vesicles and membranes. Molecular crystals and liquid crystals 202.1 (1991): 17-25.

25 Evans, Evan. Entropy-driven tension in vesicle membranes and unbinding of adherent vesicles. Langmuir 7.9

(1991): 1900-1908.

26 Rao, Madan. Active fusion and fission processes on a fluid membrane. Physical review letters 87.12 (2001): 128101.

27 Shillcock, Julian C., and Reinhard Lipowsky. The computational route from bilayer membranes to vesicle fusion. Journal of Physics: Condensed Matter 18.28 (2006): S1191.

28 Dimova, Rumiana. Recent developments in the field of bending rigidity measurements on membranes. Advances in colloid and interface science 208 (2014): 225-234.

29 Engelhardt, H., H. P. Duwe, and E. Sackmann. Bilayer bending elasticity measured by Fourier analysis of thermally excited surface undulations of flaccid vesicles. Journal de Physique Lettres 46.8 (1985): 395-400.

30 Faucon, J. F., et al. Bending elasticity and thermal fluctuations of lipid membranes. Theoretical and experimental requirements. Journal de physique 50.17 (1989): 2389-2414.

31 Pécréaux, Jacques, et al. Refined contour analysis of giant unilamellar vesicles. The European Physical Journal E 13.3 (2004): 277-290.

32 Boal, David, and David H. Boal. Mechanics of the Cell. Cambridge University Press, 2012.

33 Liu, L. P., and P. Sharma. Flexoelectricity and thermal fluctuations of lipid bilayer membranes: Renormalization of flexoelectric, dielectric, and elastic properties. Physical Review E 87.3 (2013): 032715.

34 Nelson, Philip, and Thomas Powers. Renormalization of chiral couplings in titled bilayer membranes. Journal de Physique II 3.10 (1993): 1535-1569.

35 Powers, Thomas, and Philip Nelson. Fluctuating membranes with tilt order. Journal de Physique II 5.11 (1995): 1671-1678.

36 Golestanian, Ramin, Mark Goulian, and Mehran Kardar. Fluctuation-induced interactions between rods on a membrane. Physical Review E 54.6 (1996): 6725.

37 Lin, Hsiang-Ku, et al. Fluctuation-induced forces between inclusions in a fluid membrane under tension. Physical review letters 107.22 (2011): 228104.

38 Yolcu, Cem, and Markus Deserno. Membrane-mediated interactions between rigid inclusions: an effective field theory. Physical Review E 86.3 (2012): 031906.

39 Salditt, Tim. Thermal fluctuations and stability of solid-supported lipid membranes. Journal of Physics: Condensed Matter 17.6 (2005): R287.

40 Auth, Thorsten, S. A. Safran, and Nir S. Gov. Fluctuations of coupled fluid and solid membranes with application to red blood cells. Physical Review E 76.5 (2007): 051910.

41 Xu, Wenlong, et al. Influence of counterions on lauric acid vesicles and theoretical consideration of vesicle stability. The Journal of Physical Chemistry B 117.1 : 242-251 2012

42 Zhong-Can, Ou-Yang, and Wolfgang Helfrich. Bending energy of vesicle membranes: General expressions for the first, second, and third variation of the shape energy and applications to spheres and cylinders Physical Review A 39.10 (1989): 5280.

43 Agrawal, Ashutosh, and David J. Steigmann. Boundary-value problems in the theory of lipid membranes. Continuum Mechanics and Thermodynamics 21.1 (2009): 57-82.

44 Steigmann, David J. A concise derivation of membrane theory from three-dimensional nonlinear elasticity. Journal of Elasticity 97.1 (2009): 97-101.

45 Givli, Sefi, Ha Giang, and Kaushik Bhattacharya. Stability of multicomponent biological membranes. SIAM Journal on Applied Mathematics 72.2 (2012): 489-511.

46 Walani, Nikhil, Jennifer Torres, and Ashutosh Agrawal. Anisotropic spontaneous curvatures in lipid membranes. Physical Review E 89.6 (2014): 062715.

47 Biria, Aisa, Mohsen Maleki, and Eliot Fried. Continuum theory for the edge of an open lipid bilayer. Adv. Appl. Mech 21 (2013): 1-78.

48 Fournier, J. B., Galatola, P. Tubular vesicles and effective fourth-order membrane elastic theories. EPL (Europhysics Letters), 39(2), 225 1997

49 Manyuhina, O. V., Hetzel, J. J., Katsnelson, M. I., Fasolino, A. Non-spherical shapes of capsules within a fourth-order curvature model. The European Physical Journal E: Soft Matter and Biological Physics, 32(3), 223-228 2010

50 Siegel, D. P. Fourth-order curvature energy model for the stability of bicontinuous inverted cubic phases in amphiphile– water systems. Langmuir, 26(11), 8673-8683 2010

51 Guven, J., Müller, M. M. How paper folds: bending with local constraints. Journal of Physics A: Mathematical and Theoretical, 41(5), 055203. 2008

52 Guven, J. Membrane geometry with auxiliary variables and quadratic constraints. Journal of Physics A: Mathematical and General, 37(28), L313. 2004

53 Kleinert, H. Size distribution of spherical vesicles. Physics Letters A, 116(2), 57-62. 1986

54 Föster, D. On the scale dependence, due to thermal fluctuations, of the elastic properties of membranes. Physics Letters A 114.3 (1986): 115-120.

55 Helfrich, W. Steric interaction of fluid membranes in multilayer systems. Zeitschrift Naturforschung Teil A, 33, 305. 1978

56 Peliti, L., Leibler, S. Effects of thermal fluctuations on systems with small surface tension. Physical review letters, 54(15), 1690 1985

57 Evans, E. A., and V. A. Parsegian. Thermal-mechanical fluctuations enhance repulsion between bimolecular layers. Proceedings of the National Academy of Sciences 83.19 (1986): 7132-7136.

58 May, Eric R., Atul Narang, and Dmitry I. Kopelevich. Role of molecular tilt in thermal fluctuations of lipid membranes. Physical Review E 76.2 (2007): 021913.

59 Kleinert, H. Gauge Fields in Condensed Matter. Vol. I: Superflow and Vortex Lines. World Scientific 1989

60 Kleinert, H. Path integrals in quantum mechanics, statistics, polymer physics, and financial markets. World Scientific 2009

61 Kleinert, H., Narzikulov, Z., Rakhimov, A. Quantum phase transitions in optical lattices beyond the Bogoliubov approximation. Physical Review A, 85(6), 063602 2012

62 Dreger, J., Pelster, A., Hamprecht, B. Variational perturbation theory for Fokker-Planck equation with nonlinear drift. The European Physical Journal B-Condensed Matter and Complex Systems, 45(3), 355-368 2005

63 Kleinert, H. Fluctuation pressure of membrane between walls. Physics Letters A, 257(5), 269-274 1999

64 Bachmann, M., Kleinert, H., Pelster, A. Fluctuation pressure of a stack of membranes. Physical Review E, 63(5), 051709 2001

65 Stevenson, P. M. Optimized perturbation theory. Physical Review D, 23(12), 2916 1981

66 Düttmann, M. Variational Methods in Disorder Problems. (Doctoral dissertation, Diploma Thesis), Department of Physics Freie Universitat Berlin, Berlin, Germany, 2009

67 McComb, W. D. Renormalization Methods: A Guide for Beginners. Oxford 2004

68 Palmieri, B., Safran, S. A. Hybrid lipids increase the probability of fluctuating nanodomains in mixed membranes. Langmuir, 29(17), 5246-5261 2013

69 Brewster, R., Pincus, P. A., Safran, S. A. Hybrid lipids as a biological surface-active component. Biophysical journal, 97(4), 1087-1094 2009

70 Pieruschka, P., Marčelja, S., Teubner, M. Variational theory of undulating multilayer systems. Journal de Physique II, 4(5), 763-772 1994

71 Weikl, T. R., Lipowsky, R. Adhesion-induced phase behavior of multicomponent membranes. Physical Review E, 64(1), 011903 2001

72 Ahmadpoor, Fatemeh, Liping Liu, and Pradeep Sharma. Thermal fluctuations and the minimum electrical field that can be detected by a biological membrane. Journal of the Mechanics and Physics of Solids 78 (2015): 110-122.

73 Stein, Elias M., and Guido L. Weiss. Introduction to Fourier analysis on Euclidean spaces. Vol. 1. Princeton university press, 1971.

74 Kardar, Mehran. Statistical physics of fields. Cambridge University Press, 2007.

75 Helfrich, W. Effect of thermal undulations on the rigidity of fluid membranes and interfaces. Journal de Physique, 46(7), 1263-1268 1985

76 Helfrich, W. Stiffening of fluid membranes and entropy loss of membrane closure: Two effects of thermal undulations. The European Physical Journal B-Condensed Matter and Complex Systems, 1(4), 481-489 1988

77 Kleinert, H. Thermal softening of curvature elasticity in membranes. Physics Letters A, 114(5), 263-268 1996

78 Winterhalter, M., and D. D. Lasic. Liposome stability and formation: experimental parameters and theories on the size distribution. Chemistry and physics of lipids 64.1 (1993): 35-43.

79 Korgel, Brian A., John H. van Zanten, and Harold G. Monbouquette. Vesicle size distributions measured by flow field-flow fractionation coupled with multiangle light scattering. Biophysical journal 74.6 (1998): 3264-3272.

80 Coldren, B., et al. From vesicle size distributions to bilayer elasticity via cryo-transmission and freeze-fracture electron microscopy. Langmuir 19.14 (2003): 5632-5639.

81 Egelhaaf, S. U., M. Müller, and P. Schurtenberger. Size determination of polymer-like micelles using cryo-electron microscopy. Langmuir, 14.16 : 4345-4349 1998

82 Van Zanten, Ryan, and Joseph A. Zasadzinski. Using cryo-electron microscopy to determine thermodynamic and elastic properties of membranes. Current opinion in colloid interface science 10.5 : 261-268 2005

83 Jung, H. T., et al. The origins of stability of spontaneous vesicles. Proceedings of the National Academy of Sciences 98.4 : 1353-1357 2001

84 Helfrich, W. Size distributions of vesicles: the role of the effective rigidity of membranes. Journal de Physique 47.2 (1986): 321-329.

85 Harmandaris, V. A., Deserno, M. A novel method for measuring the bending rigidity of model lipid membranes by simulating tethers. The Journal of chemical physics, 125(20), 204905 2006

86 Bo, L., Waugh, R. E. Determination of bilayer membrane bending stiffness by tether formation from giant, thin-walled vesicles. Biophysical journal, 55(3), 509-517 1989

87 Cuvelier, D., Derènyi, I., Bassereau, P., Nassoy, P. Coalescence of membrane tethers: experiments, theory, and applications. Biophysical journal, 88(4), 2714-2726 2005

88 Bar-Ziv, Roy, Thomas Frisch, and Elisha Moses. Entropic expulsion in vesicles. Physical review letters 75.19 (1995): 3481-3484.

89 Li, J., Pastor, K. A., Shi, A. C., Schmid, F., Zhou, J. Elastic properties and line tension of self-assembled bilayer membranes. Physical Review E, 88(1), 012718 2013

90 Kozlov, M. M., and W. Helfrich. Effects of a cosurfactant on the stretching and bending elasticities of a surfactant monolayer. Langmuir 8.11 (1992): 2792-2797.

91 Risselada, H. J., Marrink, S. J., Müller, M. Curvature-dependent elastic properties of liquid-ordered domains result in inverted domain sorting on uniaxially compressed vesicles. Physical review letters, 106(14), 148102. 2011